Real-Time Monitoring of Glutathione-Triggered Thiopurine Anticancer Drug Release in Live Cells Investigated by Surface-Enhanced Raman Scattering

ARTICLE *in* ANALYTICAL CHEMISTRY · MARCH 2012

Impact Factor: 5.64 · DOI: 10.1021/ac2024188 · Source: PubMed

9 AUTHORS, INCLUDING:

Erdene-Ochir Ganbold
Soongsil University
35 PUBLICATIONS **287** CITATIONS
SEE PROFILE

Jin-Ho Park
Gwangju Institute of Science and Technology
17 PUBLICATIONS **179** CITATIONS
SEE PROFILE

analytical chemistry

Article

pubs.acs.org/ac

Real-Time Monitoring of Glutathione-Triggered Thiopurine Anticancer Drug Release in Live Cells Investigated by Surface-Enhanced Raman Scattering

Kwangsu Ock,[†] Won Il Jeon,[‡] Erdene Ochir Ganbold,[†] Mira Kim,[†] Jinho Park,[†] Ji Hye Seo,[†] Keunchang Cho,[†] Sang-Woo Joo,*[,†] and So Yeong Lee*[,‡]

[†]Department of Chemistry, Soongsil University, Seoul 156-743, Korea

[‡]Laboratory of Pharmacology, College of Veterinary Medicine and Research Institute for Veterinary Science, Seoul National University, Seoul 151-742 Korea

Supporting Information

ABSTRACT: We investigated *in vitro* and *in vivo* glutathione (GSH)-induced intracellular thiopurine anticancer drug release on gold nanoparticle (Au NP) surfaces by means of label-free confocal Raman spectroscopy. Direct monitoring of GSH-triggered release of 6-mercaptopurine (6MP) and 6-thioguanine (6TG) was achieved in real time. Live cell imaging technique provides a nanomolar range release of 6MP and 6TG from Au NP surfaces after the injection of external GSH. *In vivo* SERS spectra of 6TG were obtained from the subcutaneous sites in living mice after GSH treatment. GSH-triggered releases of Cy5-dye assembled on 6TG-capped Au NPs were also compared using independent fluorescence measurements. Our work demonstrates that the time-lapse Raman spectroscopic tools are useful for monitoring of the controlled release of thiopurine drug molecules *in vitro* and *in vivo*.

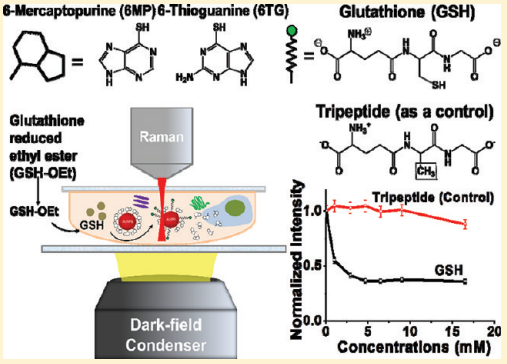

Since its discovery, surface-enhanced Raman scattering (SERS) has been widely used for biological sensing or molecular imaging near the surface of nanostructure assemblies as an ultrasensitive spectroscopic tool for interface studies.[1] The SERS method offers several advantages due to different Raman signatures for high throughput screening of various molecules with narrow bandwidths avoiding spectral overlaps along with the optical interference effects by appropriate nanostructures.[2] In addition, Raman microscopy has recently made unique contributions to the intracellular monitoring.[3−6]

Stimuli-responsive release of the pharmaceutical cargo should impact the therapeutic efficacy and cytotoxicity of drug delivery in the practical applications including chemotherapy.[7] Although numerous drug encapsulations have been developed, the release of the drugs in a controlled manner presents a challenge after the drug molecules' cellular internalization.[8] Advances in nanoparticle engineering have provided new opportunities for the therapeutic applications.[9,10] Gold nanoparticle (Au NP)-based drug delivery systems provide important tools for enhancing the efficacy of chemotherapeutics due to the low toxicity and biocompatibility.[11]

Glutathione (GSH), the most abundant thiol species at a concentration range of 1−10 mM in the cytoplasm, has been used as an *in situ* releasing reagent in living cells due to its major reducing capability in biochemical processes.[12] GSH-mediated *in vitro* release of the fluorescence dye-tagged thiol was performed for its monolayer protected Au NP surfaces.[13] Purine analogue is one of the first chemotherapy reagents to be used as an antileukemic and antineoplastic drug for the treatment of many cancer diseases.[14−18] Thiopurines are known to adsorb on Au NP surfaces through its N and S groups, and it has been shown that 6MP-modified Au NPs exhibited the enhanced drug delivery treatments of leukemia.[19] A previous work has shown that purine analogues such as 6MP efficiently adsorbed on Au NPs appear to exhibit fairly strong SERS signals.[20] Dark-field microscopy (DFM), utilizing oblique illumination and collecting the Rayleigh scattering of light, has been used to track individual nonfluorescent Au NPs.[21]

Most release studies used fluorescence techniques requiring additional dyes. This work was motivated by the fact that there are very limited label-free spectroscopic studies using Au NPs[22] on the drug release inside live cells in real time. In this work, intracellular drug release monitoring was performed using SERS and live cell imaging techniques without any use of additional tagging molecules. DFM and SERS were used to monitor desorption of 6MP or 6TG drug molecules attached onto Au NPs by means of externally supplied GSH.

Received: September 14, 2011
Accepted: January 26, 2012
Published: January 26, 2012

   dx.doi.org/10.1021/ac2024188 | *Anal. Chem.* 2012, 84, 2172−2178

EXPERIMENTAL SECTION

NP Synthesis and Characterization. The colloidal dispersions of Au NPs were prepared by the citrate reduction method.[23,24] First, 30 mL of aqueous 14 mM $HAuCl_4$ (99.9+ %, Sigma Aldrich) solution was boiled for the Au NP sample. Approximately 3 mL of 1% sodium citrate solution was then added to the $HAuCl_4$ solution under vigorous stirring, and boiling was continued for ca. 1 h. Absorption spectroscopy (Mecasys UV-3220 spectrophotometer) was used to check the surface plasmon band. The morphologies of Au NPs inside the cell were checked using a JEOL JEM-1010 transmission electron microscope. The average size of pristine Au NPs was measured to be ~20 nm by counting at least 100 particles. The quasielastic light scattering (QELS) and zeta potential measurements were used to monitor the hydrodynamic radius and the surface potential of the particles with an Otsuka ELSZ-2 analyzer. The Au percentages in NP solutions were measured to be 114 ppm (or 1.44×10^{-3} M) using a Perkin-Elmer OPTIMA 4300DV inductively coupled plasma-atomic emission spectrometer (ICP-AES). The concentration of Au NPs was estimated to be approximately 7.0×10^{-9} M by assuming ~20 nm particle size considering the atomic radius of Au is 0.14425 nm.

Materials. 6-Mercaptopurine (6MP) (>96%) and 6-thioguanine (6TG) (>95%) were purchased from Tokyo Kasei and used as received. Acycloguanosine (≥99%), allopurinol, glutathione reduced (>98%), and glutathione reduced ethyl ester (GSH-OEt, >90%) were purchased from Sigma Aldrich. Since GSH is known to be not able to internalize cell membranes due to its anionic nature, GSH-OEt was used as an external stimulus to trigger 6MP release. The tripeptide gamma glutamic acid (97%) as depicted in Figure 1 was synthesized by Peptron (Daejeon, Korea). The synthesized peptide was purified using a Shimadzu prominence HPLC equipment and tested by a Hewlett-Packard 1100 series LC-MS. The molecular weight of the tripeptide is 276.

Cell Culture. Human lung carcinoma A549 cells (ATCC CCL-185) and K562 human erythromyeloblastoid leukemia cells (ATCC CCL-243) were cultured in RPMI 1640 medium supplemented with 10% FBS and antibiotics at 37 °C in a 5% CO_2 atmosphere incubator. HeLa cells (ATCC CCL-2) were grown on DMEM. RPMI 1640 and fetal bovine serum (FBS) were obtained from WelGene (Seoul, Korea). The relative uptake amounts for each Au NP were determined by ICP-MS. A549 cells were plated at a concentration of 1×10^6 cells per dish on a 100 mm cell culture dish (SPL, KOREA) containing growth medium. NPs were added, and the cells were incubated at 37 °C with 5% CO_2. After 24 h, the cells were harvested and washed with DPBS. The samples were analyzed using a Varian inductively coupled plasma-mass spectrometer (ICP-MS).

GSH Assay. Intracellular GSH levels were measured using a fluorescence method.[25] We used a fluorescence assay kit (Sigma Catalogue #CS1020) with a Tecan F200 96 well plate reader. The kit assay utilizes a thiol probe (monochlorobimane), which can freely pass through the plasma membrane. The free, unbound probe shows very little fluorescence, but when bound to reduced glutathione in a reaction that is catalyzed by glutathione S-transferase, it forms a strongly fluorescent adduct. The microplate was then incubated at room temperature before being measured at an excitation/emission of 360/485 nm using a fluorescent plate reader. Estimation of protein was done using a bicinchoninic acid (BCA) protein assay kit (Intron Biotechnology Catalogue #21071) for the colorimetric detection and quantification of total protein using a Tecan F50 microplate reader.

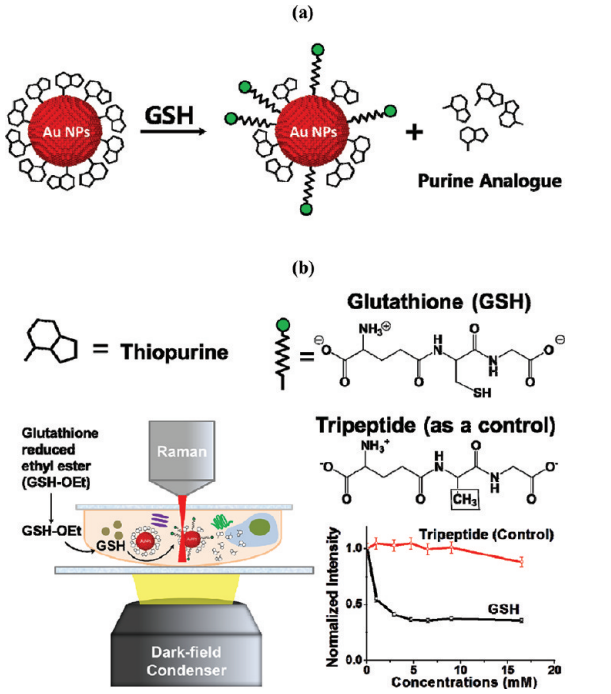

Figure 1. Experimental scheme. (a) Release of thiopurine on Au NPs via GSH. (b) *In vitro* GSH-mediated release of a part of thiopurine drug molecules adsorbed on Au NPs could be monitored thorough Raman and DFM measurements by observing a decrease in its SERS intensities in real time. Tripeptide which has a functional group of not SH but CH_3 was used as an inactive GSH derivative for a control experiment.

DFM and SERS Methods. Cellular uptake of NPs was also monitored using DFM with a Leica DL LM upright microscope and a high-resolution CytoViva 150 adapter. Our DFM resolution could be estimated from the previous literature.[26] The maximum resolution of the DFM was reported to be ~90 nm ($\lambda/5$) with a narrower diffraction limit from the annular aperture. Having the difference in magnified objective lens and CCD camera setting, our DFM resolution was estimated to be a little higher than this.

In most cases, the yellowish Au NPs can be discerned from the white color organelles in the DFM images. Raman spectra were obtained using a Raman confocal system model 1000 spectrometer (Renishaw) equipped with an integral microscope (Leica DM LM). Spontaneous Raman scattering was detected with 180° geometry using a peltier cooled (−70 °C) CCD camera (400 × 600 pixels). An appropriate holographic super-notch filter was set in the spectrometer for 632.8 nm from a 20 mW air-cooled HeNe laser (Melles Griots Model 25 LHP 928) with the plasma line rejection filter.

Live Cell Imaging. The final concentration of thiopurine at 2×10^{-4} M was used for Au NPs, and 45 μL of the mixed solution was injected into the live cell chamber (Charmlide, Korea) seeded with 2×10^5 cells. The thiopurine-coated Au NPs were incubated for ~24 h. Treated concentration of glutathione was 5−15 mM. For live cell imaging, it usually took 3−4 h in total to monitor the single cell in a chamber by obtaining the DFM image every 15−30 min and Raman spectrum every 10 min without disturbance.

dx.doi.org/10.1021/ac2024188 | *Anal. Chem.* 2012, 84, 2172−2178

Comparative Fluorescence Measurements. A volume of 200 μL of an aqueous solution containing 6TG (10^{-3} M) was added to the 20 mL of Au NP solution with vortexing for 3 min. After 20 min, a 7 mL solution containing 10 μmol of *N*-hydroxylsuccinimide (NHS)-activated Cy5 from Genechem (Daejeon, Korea) was added to the resulting dispersion which was allowed to stir at room temperature overnight in darkness. The Cy5 fluorescent probe was conjugated to the 6TG adsorbates via condensation of the NHS group of Cy5-NHS and the primary amine group of the 6TG on Au. The resulting solution was centrifuged at 17 000 rpm for 1 h, and the unreacted supernant solution was discarded. The remaining pellet was vortexed, redispered, and sonicated for 30 s in an aqueous solution and ready for the fluorescence measurement. The fluorescence emission profiles of Cy5-labeled 6TG assembled on Au NPs in living mice were obtained using a fully automated CRi MaestroTM 2 *in vivo* imaging system at the wavelength between 640 and 800 nm.

***In Vivo* Experiment.** Six week old male CAnN.Cg-Foxn1nu/CrljOri nude mice (Orient Bio Inc., Gyeonggi, Korea) were used for *in vivo* SERS spectra measurements. Au NPs (50 μL) were injected subcutaneously into the nude mice. After injection within 10 s, we attempted to observe the Raman spectrum for the skin spots of mice.[27] The band at ~1290 cm^{-1} could be observed by *in vivo* Raman experiments. 6TG-conjugated Au NPs were administered via subcutaneous injection. SERS spectra were within a few minutes after injection. *In vivo* SERS spectra of 6TG were obtained from the subcutaneous site with 25 s signal integration and at 785 nm excitation. The 6TG spectra were background subtracted by Raman spectrum of the skin. The matrigel (BD Sciences, Catalogue #356231) was used to keep the SERS-active Au NPs from diffusing quickly out of the skin.[28] We could not obtain any strong SERS signals at 632.8 nm for the *in vivo* experiment in mice. The 785 nm irradiation was used to achieve deeper penetration into the skin of the mice. Three out of tested five mice were used to obtain the *in vivo* Raman spectra. The actual 6TG spectrum was obtained after subtracting the skin background spectrum from the injected spot raw spectrum. These Raman intensities were averaged with error bars as shown in the bar graphs. We obtained Raman spectra in the order of skin, 6TG, and GSH with the acquisition time of 10 s by accumulating the spectra three times.

RESULTS AND DISCUSSION

GSH Concentration-Dependent SERS Intensities of Thiopurine Drugs. Figure 1 shows our experimental scheme of *in vitro* GSH-OEt-mediated release of a part of 6MP or 6TG drug molecules adsorbed on Au NPs by observing a decrease in its SERS intensities in real time. Glutathione monoester (GSH-OEt) was used as an intracellular external stimulus to trigger drug release.

To monitor the desorption reaction in the mammalian cells, we applied the DFM and SERS techniques. The DFM images and corresponding SERS spectra were also shown at a certain local point inside a single A549 cell after the uptake of the 6MP-modified Au NPs. The internalization of Au NPs was confirmed by z-depth dependent SERS combined with DFM. The DFM images and corresponding SERS spectra at a certain local point inside a single A549 cell after the uptake of the 6MP-modified Au NPs can confirm the internalization of NPs.

As shown in Figure 2, to check that the adsorbed 6MP appeared to be detached after the treatment of GSH, surface

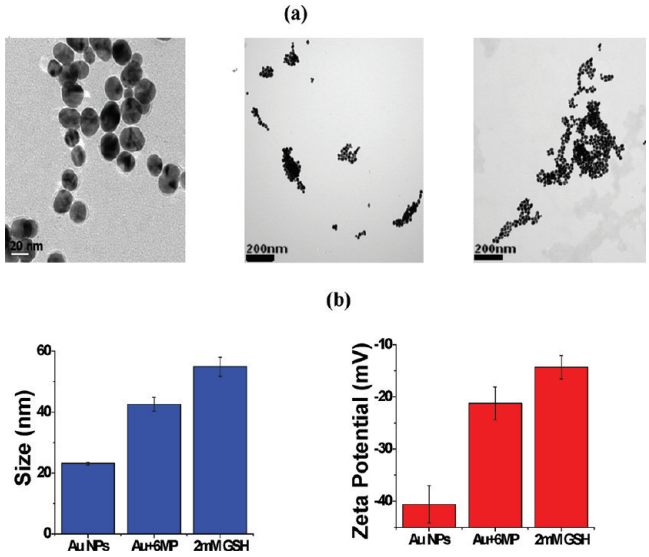

Figure 2. (a) TEM images of Au NPs, 6MP-modifed Au NPs (middle), and 6MP-coated Au NPs after 2 mM GSH treatment. The scale bars are 20, 200, and 200 nm, respectively. (b) QELS and zeta potential measurements of 6MP-modifed Au NPs, 2 mM GSH-treated 6MP-coated Au NPs, and GSH-coated Au NPs.

plasmon resonance (SPR) band, quasielastic light scattering (QELS), and zeta potential measurements indicated that GSH should replace 6MP on Au NPs. The QELS and zeta potential measurements were used to monitor the hydrodynamic radius and the surface potential of the particles. The QELS diameter profiles measuring the hydrodynamic radius of particles were measured to be 23.1 (±0.4) nm, larger than the TEM data. After coating 6MP, the aggregated size increased up to 42.6 (±2.2) nm as suggested from the plasmon shift in the absorption spectra. When we applied 2 mM GSH, the size increased to 54.9 (±3.2) nm. The zeta potential values appeared to be increased to a more positive value from −40.6 (±3.6) to −21.2 (±3.1) mV after adsorption of 6MP.

Figure 3 shows the SERS spectra of 6MP and 6TG on Au NPs in an aqueous solution depending on the amounts of GSH. The concentrations of ~10^{-5} M are close to the monolayer coverage limit at ~1.4 × 10^{-5} M considering the particle diameter and previous STM data.[29] As the concentrations of GSH were increased, the decrease in the SERS intensities of 6MP or 6TG was observed accordingly. The three independent measurements supported their reproducibility. One of the strongest vibrational bands at 1258 cm^{-1} which can be ascribed to the C−N stretching vibration[20] of the purine ring mode in 6MP was used to monitor the decrease in SERS intensities. The band at 1291 cm^{-1} was used for 6TG. The other bands of 6MP or 6TG also exhibited similar behaviors of a decrease in intensities depending on the concentration of GSH. If the tripeptide was used instead of GSH as an inactive GSH derivative for a control experiment, such a decrease in the SERS signals of 6MP and 6TG was not observed.

As shown in Figure 4a,b, TEM images indicated an intracellular distribution of aggregated Au NPs in both A549 and K562 cells. TEM images indicated that 6MP-coated Au NPs were mostly found as an aggregated form inside the vesicular structures (endosomes or lysosomes) that could be ascribed to the receptor-mediated endocytosis. Colocalization of Cy5-tagged 6TG-coated Au NPs with the lysosome indicated that 6TG-coated Au NPs and lysosomes exhibited significant

dx.doi.org/10.1021/ac2024188 | *Anal. Chem.* 2012, 84, 2172−2178

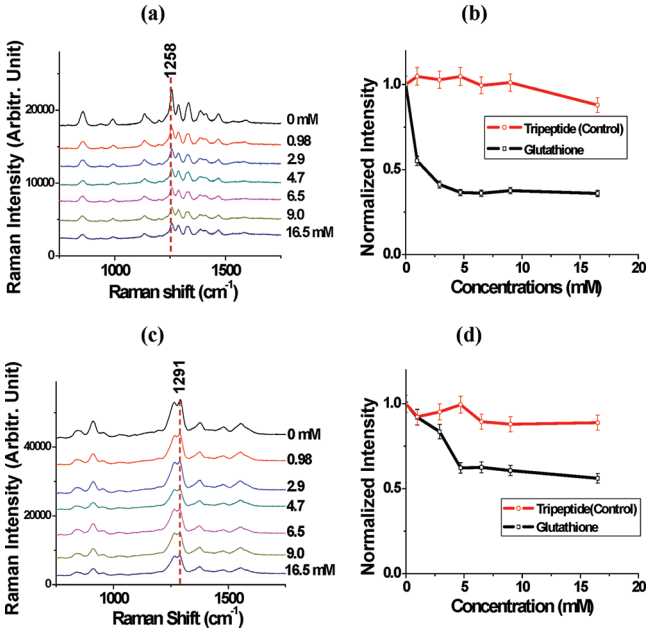

Figure 3. GSH concentration-dependent SERS intensities of (a) 6MP ($\sim 10^{-5}$ M) and (c) 6TG ($\sim 10^{-5}$ M) on Au NP surfaces in an aqueous solution. Plots of decrease in the band intensities depending on the GSH and tripeptide concentrations. The error bars indicate the standard deviation of the three measurements. The peaks at (b) 1258 and (d) 1291 cm^{-1} were used to compare the relative intensities from 6MP and 6TG, respectively. Tripeptides with the same concentration of GSH (>5 mM) were used as a control. Raman spectra were obtained after a few minutes from the injection time of peptides.

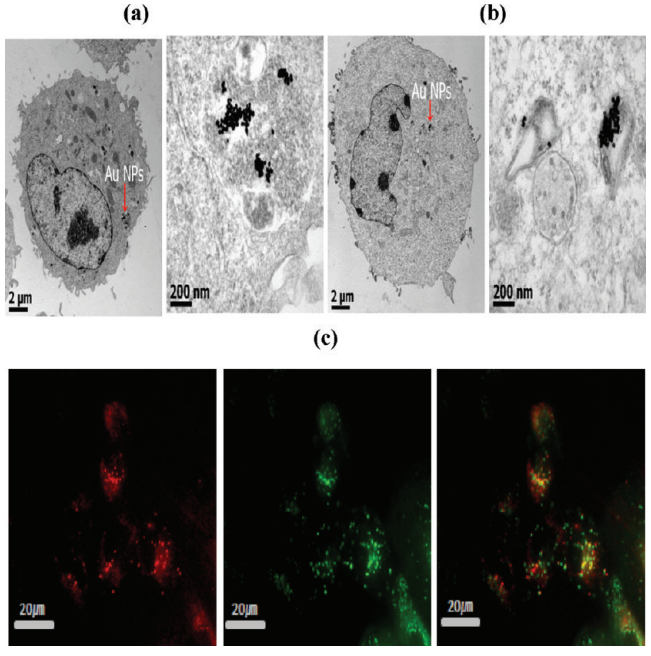

Figure 4. TEM images of 6MP-modifed Au NPs and its magnified view in (a) an A549 and (b) a K562 cell. (c) Colocalization of Cy5-tagged 6TG-coated Au NPs (left), lysosome (middle), and their overlapped images (right). 6TG-coated Au NPs and lysosomes exhibited significant overlaps in their fluorescence images.

overlaps in their fluorescence images as suggested in Figure 4c. Although the cellular uptakes of 6MP-coated and Cy5-tagged 6TG-coated Au NPs were checked, only static information was provided through these TEM and fluorescence images. To monitor the real-time release of 6MP and 6TG from the Au NP surfaces, we performed a Raman spectroscopic study with a combination of the DFM technique[21] equipped with a live cell chamber.

Time-Lapse DFM Live Cell Images in a Single A549 Cell. Figures 5 and 6 show real-time time-lapsed live cell

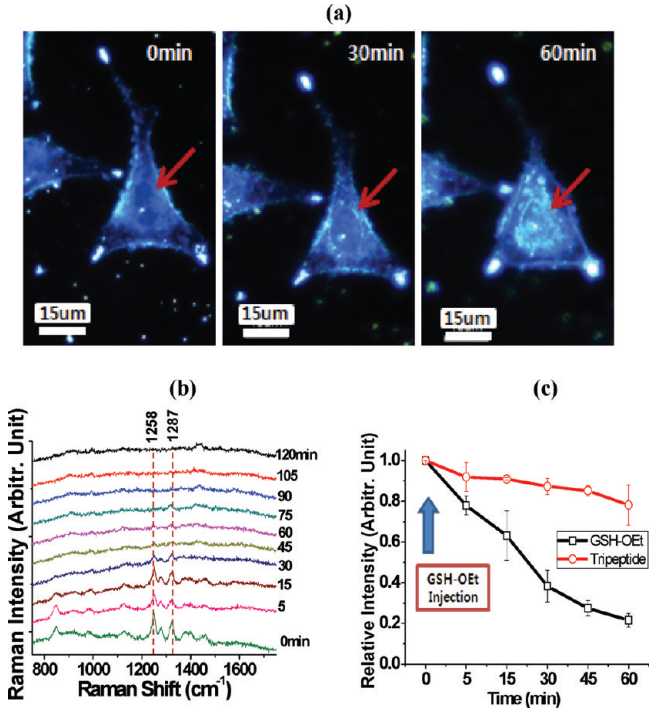

Figure 5. (a) Time-lapse DFM live cell images in a single A549 cell after treatment of glutathione ethyl ester (GSH-OEt) indicating the *in situ* release of 6MP from Au NPs. The arrow indicates the position where the Raman spectra were obtained. The Au NPs were incubated for 24 h prior to the GSH-OEt treatment. (b) The peak at 1258 cm^{-1} was monitored with time. The other vibrational bands of 6MP also showed similar behaviors. Raman spectra were obtained after a few minutes from the injection time of GSH-OEt. (c) Plot of decrease in the band intensities depending on the elapsed time after GSH-OEt injection. The error bar indicated the standard deviation of the three measurements. GSH-OEt and tripeptides were marked in black and red, respectively.

imaging data of 6MP and 6TG, respectively. It was possible to observe the release of thiopurine drugs using intracellular endogenous GSH after sufficient elapsed time. Due to the cell movements and varying physiological conditions in the cellular medium, it was difficult to judge whether the decrease in the SERS intensities should be ascribed not to any cell morphological changes but to the intended drug release, as the monitoring time became longer. Under our experimental condition, 3−4 h is the total acquisition time for a live-cell imaging experiment by maintaining the uniform conditions without affecting the cellular medium significantly. Since we intended to observe an immediate response to drug release within 3−4 h, we infused a concentration of GSH-OEt higher than 5 mM into the cell medium. A prompt drop in Raman intensity within a 10 min period could be observed by applying such a high concentration of externally supplied GSH-OEt. Independent fluorometric assay[25] indicated that the intracellular GSH increased by 40% within 90 min, if we injected

dx.doi.org/10.1021/ac2024188 | *Anal. Chem.* 2012, 84, 2172−2178

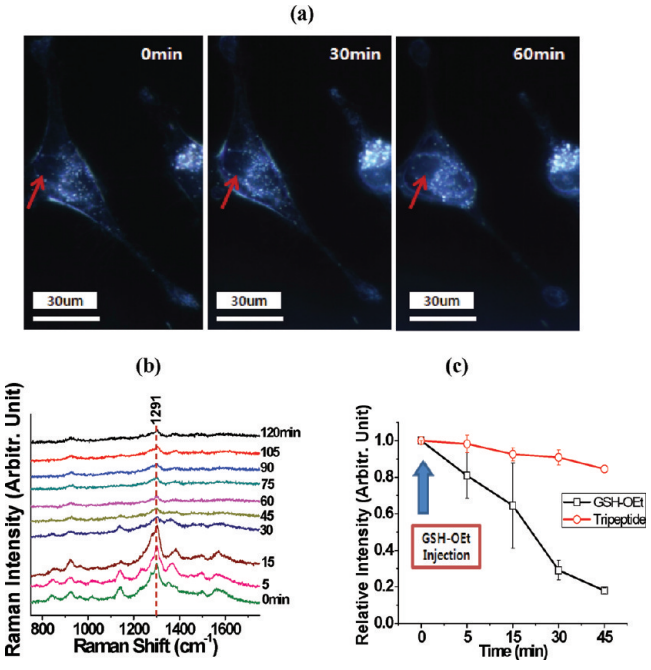

Figure 6. (a) Time-lapse DFM live cell images in a single HeLa cell after treatment of glutathione ethyl ester (GSH-OEt) indicating the *in situ* release of 6TG from Au NPs. The arrow indicates the position where the Raman spectra were obtained. (b) The strongest peak at 1291 cm^{-1} from 6TG was used. (c) Plot of decrease in the band intensities depending on the elapsed time after GSH-OEt injection.

GSH-OEt as high as 15 mM into the cellular medium. The LC MS/MS data also supported that the intracellular GSH levels should be around 2 mM within an hour after the treatment of >5 mM GSH-OEt. According to our ICP-MS data, the uptake rate of Au NPs into the cells was measured below a few percent (~0.25%) consistent with the recent report.[30] The concentrations of Au NPs and attached 6MP inside the cells were thus estimated to be 1.8×10^{-11} and 3.6×10^{-8} M, respectively, inside the cell. From our Raman measurements, approximately 1.8×10^{-9} M of 6MP release could be monitored by measuring its Raman peaks with a signal-to-noise ratio of ~10 by optimizing our experimental conditions in our live cell chamber.

Considering that the IC_{50} values of 6MP and 6TG were reported to be in the micromolar range,[19,31] our method should be practically applicable to the physicological experiments. When GSH-OEt was injected into the cell, we could observe an approximately 40−70% decrease in the SERS intensities suggesting the release of the 6MP or 6TG drug molecules from the surfaces of Au NPs. It has to be mentioned that the SERS intensities depending on the adsorbate molecules and the geometry of nanostructures including hot spots are not in proportion to the surface coverage.[32,33] After the treatment of 5 mM GSH and subsequent centrifugation, the amount of 6MP released into the supernatant solution was estimated by UV measurements as referred from the previous report of gemcitabine on gold nanoparticles.[34] After treating with 5 mM GSH, the 6MP adsorbates were found to be released by ~40% (see Supporting Information), whereas the SERS intensities dropped by ~70% as shown in Figure 3a,b. Although the property of Au NPs to aggregate inside cells may give higher local concentrations and field strength, our SERS signals can provide the relative intensity change caused by GSH-mediated release. Live cell imaging techniques combined with Raman spectroscopy can be a useful tool in the stimulated release of drug molecules. It has to be mentioned that the SERS intensities depending on the adsorbate molecules and the geometry of nanostructures including hot spots are not in proportion to the surface coverage.[32,33] We have performed the UV−vis absorption spectra that GSH actually released the adsorbates and can be compared with the SERS intensities in a quantitative way.

We are currently extending our methods of GSH-triggered drug release to other nonthiol drugs for more versatile applications. Acycloguanosine and allopurinol, which are non-thiol-containing drugs, exhibited similar behavior in solution, but showed weaker SERS intensities than 6MP and 6TG even in GSH-deficient cell lines after treatment with buthionine sulphoximine, although the data are not shown here. This may be due to the weaker binding of acycloguanosine and allopurinol than 6MP and 6TG. It is expected that the nitrogen containing drug compounds may detach easily in cytosols by intracellular GSH, whereas 6MP and 6TG attached on Au NPs can show strong SERS intensities inside an endosome or a lysosome.

Comparative Fluorescence Measurements. To further confirm GSH-triggered Raman signal drop, we used independent fluorescence measurements. After conjugating the Cy5 dye onto the 6TG-coated Au NPs, the fluorescence recovery was found by GSH. Such recovery was not observed by tripeptide as a control. These results indicated that the thiol group of GSH should be responsible for releasing the 6TG drug molecules. Although not shown here, we could not observe any fluorescence signals for Cy5-conjugated 6TG drug due to the quenching effect of Au NPs (see Supporting Information). The fluorescence of Cy5 became observed in an hour after treatment with greater than 5 mM GSH-OEt. These results supported that the thiol group of GSH should be responsible for releasing the thiopurine drugs in Raman experiments. Nanometal surface energy transfer, an energy transfer process from optically excited organic fluorophores to small metal nanoparticles with d^{-4} distance dependence,[35] obeys different enhancement mechanisms from SERS.

Figure 7 shows *in vitro* and *in vivo* fluorescence images of Cy5-dye (3×10^{-8} M) assembled on 6TG-capped Au NP by using GSH-OEt (>5 mM) as an external stimulus in A549 cells. The Au NPs were incubated for 24 h prior to the GSH-OEt treatment. Stick diagram of fluorescence intensities by flow cytometry analysis is also shown in Figure 7a. *In vivo* fluorescence image of Cy5-dye assembled on 6TG-capped Au NPs (50 μL) was also obtained after a subcutaneously injection to a mouse with or without GSH (16 μL, 80 mM). Stick diagram of relative intensities with or without GSH is also shown in Figure 7b.

***In Vivo* Raman Measurements of Mice.** Although our Raman experiments were focused on the *in vitro* drug release, *in vivo* SERS detection was attempted by using anticancer drug-conjugated Au NPs. SERS spectra were obtained within a few minutes after injection. Figure 8a illustrates a laser beam focusing on the injected site. *In vivo* SERS spectra of 6TG were obtained from the subcutaneous site with 25 s signal integration and at 785 nm excitation. The spectra from the skin were background subtracted. When we used the matrigel, we could manage to tell the difference for the strongest band of 6TG after treating with GSH. Figure 8 shows the *in vivo* Raman experiments exhibiting one of the strongest peaks in 6TG at

dx.doi.org/10.1021/ac2024188 | *Anal. Chem.* 2012, 84, 2172−2178

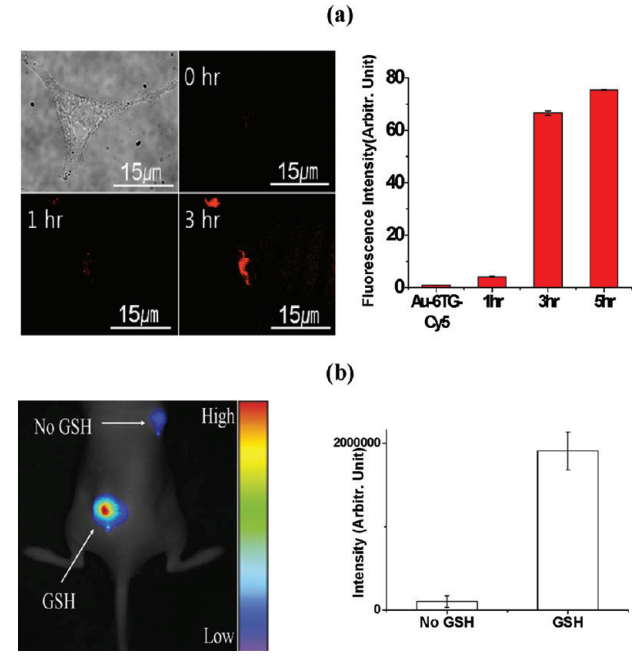

Figure 7. (a) *In vitro* fluorescence images of Cy5-dye (3×10^{-8} M) assembled on 6TG-capped Au NPs by using GSH-OEt (>5 mM) as an external stimulus in a single A549 cell. (b) In vivo fluorescence image of Cy5-dye assembled on 6TG-capped Au NPs (50 mL) subcutaneously injected to a mouse with or without GSH (16 mL, 80 mM).

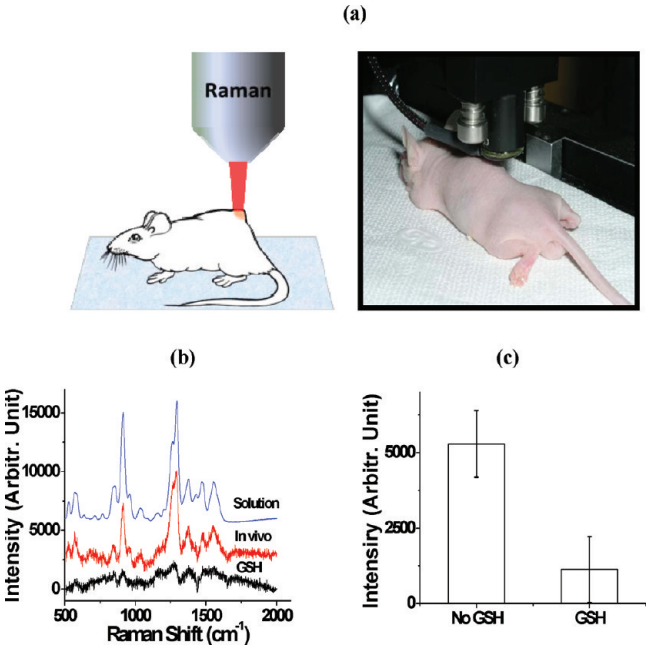

Figure 8. (a) *In vivo* experimental configuration and photograph showing a laser beam focusing on the injected site of anticancer-coated Au NPs. (b) The peaks of 6TG appeared to be much stronger than the case after GSH treatment. A volume of 50 μL of matrigel and 6TG-coated Au NP solution was injected first with a ratio of 1:1. GSH (40 mM) was subsequently injected with a volume of 30 μL. (c) Stick diagram of relative intensities with or without GSH.

1291 cm^{-1}. This band appeared to decrease when GSH-OEt was treated, whereas the control tripeptide did not show much influence. It would be possible to apply our method by introducing an appropriate functionalization and increasing the sensitivity. Moreover, our 6MP-coated Au NP systems did not cause any acute toxicity but reduced the tumor volumes after intratumoral injection to the HeLa cells xenografted to nude mice for a treatment period of two weeks.

CONCLUSIONS

We directly monitored the glutathione-induced *in vitro* and *in vivo* thiopurine anticancer drug release from Au NP surfaces by means of label-free Raman spectroscopy. A live cell imaging technique provides a nanomolar range release of thiopurine from Au NP surfaces after the injection of external glutathione. *In vivo* SERS spectra of 6TG were obtained from the subcutaneous site in living mice after treating with GSH. Our work demonstrates that the time-lapse Raman spectroscopic tools are useful for monitoring of the controlled release of thiopurine drug molecules from Au NPs inside living cells.

ASSOCIATED CONTENT

Supporting Information

Additional material as noted in the text. This material is available free of charge via the Internet at http://pubs.acs.org.

AUTHOR INFORMATION

Corresponding Author

*Phone: +82-2-8801283. Fax: +82-2-8790378. E-mail: sjoo@ssu.ac.kr, leeso@snu.ac.kr.

Notes

The authors declare no competing financial interest.

ACKNOWLEDGMENTS

We acknowledge the financial support from the NRF (2011-0001316, 2011-0027696) and the Development of Characterization Techniques for Nanomaterials Safety Project of KRCF. We would like to thank Prof. Sung Ik Yang for valuable help of in vivo Raman measurements.

REFERENCES

(1) Pallaoro, A.; Braun, G. B.; Reich, N. O.; Moskovits, M. *Small* **2010**, *6*, 618−622.
(2) Shoute, L. C.; Bergren, A. J.; Mahmoud, A. M.; Harris, K. D.; McCreery, R. L. *Appl. Spectrosc.* **2009**, *63*, 133−140.
(3) Pully, V. V.; Lenferink, A.; van Manen, H. J.; Subramaniam, V.; van Blitterswijk, C. A.; Otto, C. *Anal. Chem.* **2010**, *82*, 1844−1850.
(4) Boyd, A. R.; McManus, L. L.; Burke, G. A.; Meenan, B. J. *J. Mater. Sci.: Mater. Med.* **2011**, *22*, 1923−1930.
(5) Zong, S.; Wang, Z.; Yang, J.; Cui, Y. *Anal. Chem.* **2011**, *83*, 4178−4183.
(6) Zachariah, E.; Bankapur, A.; Santhosh, C.; Valiathan, M.; Mathur, D. *J. Photochem. Photobiol., B* **2010**, *100*, 113−116.
(7) Choi, S. W.; Zhang, Y.; Xia, Y. *Angew. Chem., Int. Ed.* **2010**, *122*, 8076−8080.
(8) Sauer, A. M.; Schlossbauer, A.; Ruthardt, N.; Cauda, V.; Bein, T.; Bräuchle, C. *Nano Lett.* **2010**, *10*, 3684−3691.
(9) Petros, R. A.; DeSimone, J. M. *Nat. Rev. Drug Discovery* **2010**, *9*, 615−627.
(10) Vivero-Escoto, J. L.; Slowing, I. I.; Wu, C.-W.; Lin, V.S.-Y. *J. Am. Chem. Soc.* **2009**, *131*, 3462−3463.
(11) Cobley, C. M.; Chen, J.; Cho, E. C.; Wang, L. V.; Xia, Y. *Chem. Soc. Rev.* **2011**, *40*, 44−56.
(12) Lee, R.; Britz-McKibbin, P. *Anal. Chem.* **2009**, *81*, 7047−7056.
(13) Hong, R.; Han, G.; Fernández, J. M.; Kim, B-j.; Forbes, N. S.; Rotello, V. M. *J. Am. Chem. Soc.* **2006**, *128*, 1078−1079.
(14) Elion, G. B. *Science* **1989**, *244*, 41.
(15) Cheok, M. H.; Evans, W. E. *Nat. Rev. Cancer* **2006**, *6*, 117−129.

(16) Tili, E.; Michaille, J. J.; Wernicke, D.; Alder, H.; Costinean, S.; Volinia, S.; Croce, C. M. *Proc. Natl. Acad. Sci. U.S.A.* **2011**, *108*, 4908−4913.
(17) Coulthard, S. A.; Redfern, C. P.; Vikingsson, S.; Lindqvist-Appell, M.; Skoglund, K.; Jakobsen-Falk, I.; Hall, A. G.; Taylor, G. A.; Hogarth, L. A. *Mol. Cancer Ther.* **2011**, *10*, 495−504.
(18) Ren, X.; Li, F.; Jeffs, G.; Zhang, X.; Xu, Y. Z.; Karran, P. *Nucleic Acids Res.* **2010**, *38*, 1832−1840.
(19) Podsiadlo, P.; Sinani, V. A.; Bahng, J. H.; Kam, N. W. S.; Lee, J.; Kotov, N. A. *Langmuir* **2008**, *24*, 568−574.
(20) Szeghalmi, A. V.; Leopold, L.; Pinzaru, S.; Chis, V.; Silaghi-Dumitrescu, I.; Schmitt, M.; Popp, J.; Kiefer, W *J. Mol. Struct.* **2005**, *735*, 103−113.
(21) Park, J.-H.; Park, J.; Dembereldorj, U.; Cho, K.; Lee, K.; Yang, S. I.; Lee, S. Y.; Joo, S.-W. *Anal. Bioanal. Chem.* **2011**, *401*, 1635−1643.
(22) Shah, N. B.; Dong, J.; Bischof, J. C. *Mol. Pharm.* **2011**, *8*, 176−184.
(23) Lee, P. C.; Meisel, D. *J. Phys. Chem.* **1982**, *86*, 3391−3395.
(24) Park, J.; Park, J. H.; Ock, K. S.; Ganbold, E. O.; Song, N. W.; Cho, K.; Lee, S. Y.; Joo, S. W. *J. Colloid Interface Sci.* **2011**, *363*, 105−113.
(25) Clift, M. J.; Boyles, M. S.; Brown, D. M.; Stone, V. *Nanotoxicology* **2010**, *4*, 139−149.
(26) Vainrub, A.; Pustovyy, O.; Vodyanoy, V. *Opt. Lett.* **2006**, *31*, 2855−2857.
(27) Qian, X.; Peng, X. H.; Ansari, D. O.; Yin-Goen, Q.; Chen, G. Z.; Shin, D. M.; Yang, L.; Young, A. N.; Wang, M. D.; Nie, S. *Nat. Biotechnol.* **2008**, *26*, 83−90.
(28) Keren, S.; Zavaleta, C.; Cheng, Z.; de la Zerda, A.; Gheysens, O.; Gambhir, S. S. *Proc. Natl. Acad. Sci. U.S.A.* **2008**, *105*, 5844−5849.
(29) Pensa, E.; Carro, P.; Rubert, A. A.; Benítez, G.; Vericat, C.; Salvarezza, R. C. *Langmuir* **2010**, *26*, 17068−17074.
(30) Ponti, J.; Colognato, R.; Franchini, F.; Gioria, S.; Simonelli, F.; Abbas, K.; Uboldi, C.; Kirkpatrick, C. J.; Holzwarth, U.; Rossi, F. *Nanotoxicology* **2009**, *3*, 296−306.
(31) Miron, T.; Arditti, F.; Konstantinovski, L.; Rabinkov, A.; Mirelman, D.; Berrebi, A.; Wilchek, M. *Eur. J. Med. Chem.* **2009**, *44*, 541−550.
(32) Le Ru, E. C.; Etchegoin, P. G. *J. Chem. Phys.* **2009**, *130*, 181101.
(33) Fang, Y.; Seong, N. H.; Dlott, D. D. *Science* **2008**, *321*, 388−392.
(34) Patra, C. R.; Bhattacharya, R.; Wang, E.; Katarya, A.; Lau, J. S.; Dutta, S.; Muders, M.; Wang, S.; Buhrow, S. A.; Safgren, S. L.; Yaszemski, M. J.; Reid, J. M.; Ames, M. M.; Mukherjee, P.; Mukhopadhyay, D. *Cancer Res.* **2008**, *68*, 1970−1978.
(35) Yun, C. S.; Javier, A.; Jennings, T.; Fisher, M.; Hira, S.; Peterson, S.; Hopkins, B.; Reich, N. O.; Strouse, G. F. *J. Am. Chem. Soc.* **2005**, *127*, 3115−3119.